X CONGRESSO NACIONAL DE ENGENHARIA MECÂNICA 2018
ABCM
20 A 24 DE MAIO DE 2018 SALVADOR – BA – BRASIL

Scramjet Analytical Flowpath Characterization Software: A preliminary study for the 14-X BS Hypersonic Engine

Emersson David Costa Claro do Nascimento, emersson11@gmail.com[1]
Israel da Silveira Rêgo, israel.rego@ieav.cta.br[1]

[1] Institute for Advanced Studies – IEAv/DCTA, Trevo Coronel Aviador José Alberto Albano do Amarante, 01 - Putim, São José dos Campos - SP, 12228-001, Brasil.

Summary: This work presents preliminary results for a beta software capable of analytically estimate the following flowpath properties for flat-plate leveled scramjets under shock-on-lip-on-corner conditions: 1.Static Pressure; 2.Static Temperature; 3.Specific Mass; 4.Mach Number; 5.Ground Speed; 6.Speed Speed; 7.Reynolds Number; 8.Shock Waves; 9. Expansion Waves; 10.Wave drag; 11.Skin-Friction Drag, 12.Pressure Thrust and 13.Resulting Pressure Force. The software is applicable in design reviews and mission architecture analysis, as it allows investigations on the forces and properties acting on the flow as a function of the scramjet geometry, helping to refine its propulsion system, for different designs, altitudes and cruising speeds. The method involves the modeling and processing segmentation of the flow in viscous nucleus and non-viscous nucleus, added to the detachment of the boundary layer between each shock and expansion wave generated. The non-viscous nucleus is considered as a quasi-unidimensional Eulerian flow, according to the Shock-Expansion Theory with confined expansion. The viscous nucleus is then treated, considering near-wall effects on compressible laminar flow at smooth flat plates with zero gradient pressure in the direction normal to the walls. The results were obtained through a case study of the 14-X BS Scramjet engine, under development at the Institute for Advanced Studies, to demonstrate scramjet technology under Mach 7 at 30 km altitude AMSL. A graphical interface was developed for Microsoft Excel 2016, aiming to take advantage of its user capillarity, facilitating engineering analysis and the identification of critical aerothermodynamic events in the hypersonic engine geometry. The interface can be used by other simulations, by simply feeding a database in a predefined format. Once the software reaches an appropriate technology readiness level, it may increase the efficiency of preliminary design reviews for any future flat plate scramjet, increasing the agility of engineering and mission decisions. The software is being developed to allow future integrations with artificial inteligence algorithms that optimize scramjets analysis for different flight trajectory and launch vehicles.

Palavras-chave: *Propulsion, Hypersonic, Scramjet, 14-X, Space*

1. INTRODUCTION

The international space sector has an increasing tendency to the development of space access technologies and mission architectures that presents safer and more economical alternatives than those provided by conventional rockets, as it can be observed by the ascension of projects such as the renewable stages of the Falcon 9, from SpaceX (SpaceX, 2015), and the New Shepard vehicle, from Blue Origin (Blue Origin, 2017).

To meet those challenges and obtain vanguard positions in the sector, the Brazilian Air Force, through its Institute for Advanced Studies, conceived the 14-X Aerospace Hypersonic Vehicle project: a platform for technology demonstration, that uses scramjet engines as its propulsion system (Nascimento et al., 2013).

Scramjets are aerospace engines that aspirate atmospheric air to use it as oxidizer at supersonic combustions. Those engines could boost renewable aerospace vehicles through suborbital hypersonic flights. Scramjet technology has greater specific impulses at hypervelocities when compared to ramjet systems and conventional rocket engines. They are advantageous in relation to conventional rocket technology, because they can use less fuel to generate longer thrust and they meet high speed operation requirements (Mach > 5) more cost-effectively and with greater safety and reliability (Heiser & Pratt, 1994).

The test model 14-X BS aims to help developers to master the flow behavior within the scramjet, before a vehicle waverider technology (Curran & Murthy, 2000; Galvão & Toro, 2013) can be further pursued. The 14-X BS (see Figs. 1 and 2) has a mirrored configuration, composed by two reflected identical scramjets. Each scramjet has two compression ramps, to provide appropriate supersonic combustion conditions at the engines combustors, and two posterior expansion ramps, to generate the expected thrust.

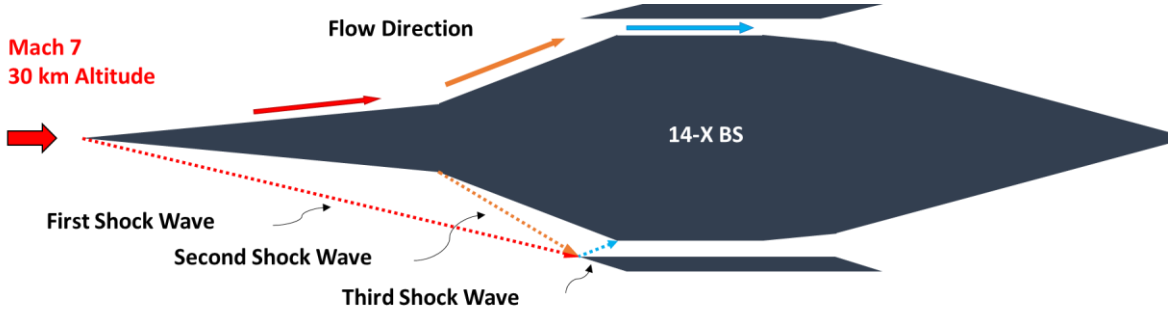

Figure 1 - Schematic illustration of the 14-X BS shock waves and streamlines. (Adaptation of Cardoso, 2012).

In hypersonic flow studies involving airfoils, as in the 14-X BS, five types of aerothermodynamic drags are considered (Anderson, 2011): 1. Wave drag; 2.a. Skin-Friction drag on laminar boundary layer; 2.b. Skin-Friction drag on turbulent boundary layer; 3. Pressure drag; 4. Lift-Induced Drag; and 5. Shock-Induced Drag. The present study investigates types 1 and 2.

The present authors are developing a software capable of characterize the 14-X BS scramjet flowpath as a function of its geometry, speed and altitude. The software output consists in: 1. The arrangement of shock/expansion waves along the scramjet; 2. The main aerothermodynamic characteristics of the flow between them; and 3. The wave drag, skin-friction drag and thrust forces acting in the scramjet.

The present work aims to share the current development stage of this software alongside with its preliminary results obtained for the 14-X BS model, under conditions of leveled cruise flight at 30 km of altitude and Mach 7.

Through the research being developed here, together with other works in progress at the Institute for Advanced Studies, it is sought to determine the total drag generated by the 14-X BS, which will allow to calculate the thrust required to its propulsion system, during flight, and further design review the hypersonic engine.

2. METHODOLOGY

2.1. Flow Segmentation

In order to make the theoretical and computational treatment feasible, the flow is modeled in two distinct segments: non-viscous nucleus (or freestream) and viscous nucleus (or boundary layer). First, the freestream is characterized and then, its function, the boundary layer is further characterized.

2.2. Freestream or non-viscous nucleus

The freestream (White, 2011) is modeled as a non-viscous, quasi-unidimensional Eulerian isentropic flow (Anderson, 2011; Emersson and Rêgo, 2017), where the variations of the aerothermodynamic properties in orthogonal directions downstream are very small when compared to gradients parallel to it.

The mathematical treatment considers a freestream in permanent regime, composed of heat-perfect gas, whose tangential direction of the flow velocity is always adjusted to the walls by the deflection caused by shock / expansion waves. Furthermore, any orthogonal components of freestream velocity relative to their tangential do not generate momentum in the flow (Anderson, 2011).

The mathematical treatment used in this study recognizes the gain of entropy by the flow in the internal region of the shock / expansion waves. However, the interaction of the flow with this region does not influence the mathematical relationships already found in (Nascimento and Rêgo, 2017) to correlate the aerothermodynamic properties before and after each shock wave and expansion.

In addition, it is considered that the angles between the 14-X BS ramps are small enough (Cardoso, 2012) not to generate shock / expansion wave detachment. Therefore, the freestream flows over the geometry of the vehicle through a series of oblique shock and expansion waves, according to the "Shock-Expansion Theory" for supersonic airfoils (Anderson, 2011).

Finally, the confined expansion model (Anderson, 2011) is used to treat the freestream in expansion ramps. For this, the flow is considered to be confined to a geometry symmetrically mirrored to each expansion ramps, relative to the axis of symmetry of the combustor, as predicted in CFD analyzes (Cardoso et al, 2013).

2.3. Boundary layer or viscous nucleus

After the freestream characterization, the boundary layers are modeled as separate systems for each region between shock/expansion waves, where specific near-wall effects for viscous laminar flows in hypersonic and supersonic regimes are considered. Thus, non-slip flow conditions are considered, when in contact with the walls, to obtain the boundary layer shear stress and flow velocity profiles (White, 2011). Moreover, aerothermodynamic properties at the interface between freestream and boundary layer are equal. This contour condition, therefore, allows an appropriate integration between the two flow segments.

The boundary layer is modelled as a steady-state flow composed of a perfectly heat gas, whose tangential direction downstream of the flow is always adjusted to the deflection caused by shock / expansion waves.

This study also adopts the constant pressure simplification along the normal direction of the flow in boundary layers. It is emphasized that this is a common model for hypersonic systems, adopted here for the sake of simplification, but which, in highly hypersonic regimes, is not always valid (Anderson, 2006).

One could argue that the boundary layer would act as virtual geometry, where the freestream would be forced to deflect along its thickness. Consequently, the effective elevation angle of the scramjet ramps would be modified by the viscous nucleus thickness, which would, therefore, modify the shock and expansions waves strength. However, the deflection angle and wave strength variation are sufficiently small to be disregarded at this stage of software development.

Likewise, at the occurrence of shock or expansion waves, the study models a detached boundary layer, such that, after each wave, a new layer is formed, as a function of its adjacent freestream, downstream of the wave. Therefore, it is modeled for this study that the bounded layer exerts no influence on the freestream, other than the generation of skin-friction drag in the hypersonic engine.

At those conditions, the viscous nucleus mathematical treatment follows the Van Driest (1952) laminar boundary layer theory in compressible fluids using the Crocco Method, alongside with the Blasius theory for flat plate laminar boundary layer profiles (White, 2011).

2.4. Combustion and reactivity

It should be noted that this study does not consider effects of heat addition, caused by supersonic combustion in the scramjet engine. The study also does not consider effects of reactive flow or radical formation. All calculations are made for the same mixture of air, not discretized the different chemical compounds that compose it.

2.5. Aerothermodynamic forces of interest

At the present software development stage, the study considers four internal forces: 1.Wave drag or pressure drag; 2.Skin-friction drag; 3.Pressure thrust; and 4.Horizontal resultant force (R). The forces are calculated only for their respective horizontal components.

Forces 1 and 3 are considered pressure forces, i.e., forces culminating from the static pressure influence in a finite area. All pressure forces contrary to the nominal direction of movement of the engine were considered as wave drag forces, while all pressure forces in favor of the vehicle motion were considered as pressure thrust (Anderson, 2011). It is important to note that pressure thrust is only one component of the total thrust of the engine. The force 2 is considered a surface force, i.e. force due to shear stress between the flow and the engine walls.

It is important to clarify that, as the gas molecules collide elastically with a surface, they transfer their momentum to this surface. In this way, the linear momentum of a gas is a mean summation of the linear momentum of its molecules. Similarly, with each collision, the molecules exert a force on their respective shock section, pressing this surface. Analogously, a mean summation of these pressures over a total surface area is its total gas pressure. In this way, when calculating the pressure thrust, for each infinitesimal length of the flow, it is accounted for the pressure gradient along the hypersonic engine flow and, therefore, for its momentum variation.

2.6. Coding, modularity and computational logic

The software is being coded in Python, a high-level, open-sourced modern language that do not generate costs for the IEAv and allows a high level of integration with any other software being developed by the Institute and a future complementary work with machine learning and artificial intelligence.

The software has a modular logic, by which the processing of the equations that compose it, occurs in independent modules. This allows that, by refining the calculating method of some physical mechanism, this refinement can be included in the software without the need for full code recoding.

The program divides the scramjet into 1000 parts along its length at its x--axis. It then processes the free flow, generating all related values, for each value of x. After this processing, the program returns to the beginning of the scramjet length and, for each section of the flow between shock or expansion waves, the program processes the boundary layer, for each value of x. Thus, the viscous nucleus processing does not change the generated values for the non-viscous one.

2.7. Database

Once the software is complete, the user will be able to choose from a list of scramjets, Mach's and altitudes available in the developed Graphical User Interface (GUI). This list is intended to include all IEAv scramjets, including 14-X BS, 14-X (Costa et al, 2013) and 14-X B, in addition to other major flat plate scramjets already published in the international literature. These filters are fed by the database, located directly in the Excel file of the GUI itself. This, in turn, is generated by the software in Python. Thus, the intention is that, once the database has a sufficient number of simulated scenarios, the user limits himself to the GUI for his analyzes. The generated database is composed of 57 variables.

2.8. Integration with other simulations

Other simulations can feed the database with its own data, just by following the same formatting. With this, their data can also be analyzed through the GUI. The modularity of the computational logic also allows new calculations to be inserted in the Python code, without prejudice to the rest of the coding. Thus, even simulations from other forms of CFD could, in principle, be executed and analyzed with the same structure.

2.9. Limitations

Currently, the software needs the manual input of the scramjet geometry, cruise Mach number and cruise altitude to begin its processing.

In addition, the software is not yet capable of automatically simulating wave reflection. For this reason, the shock-on-lip-on-corner condition is implemented manually, enabling appropriate conditions for this analysis. Likewise, fairing effects at the flow are also implemented directly in software coding.

As the modeling of this software resides in a fundamentally integral analysis (Nascimento and Rêgo, 2016), phenomena of a discretized nature - such as the confinement of expanding gases (Anderson 2011) as a result of effects of virtual geometry (Nascimento et al., 2013) - were manually modeled for expansion ramps, based on predictions of CFD analyzes already performed for the 14-XB Scramjet (Cardoso et al., 2013).

The software is only valid for cruise conditions, in steady state, under zero angle of attack. Also, it is reinforced that the present modeling still does not consider effects of heat addition by supersonic combustion. The laminar boundary layer hypothesis is also limited.

It should be noted that the graphical user interface also has its limitations. The Office Excel software installation is necessary, and when the database is too large, Excel may become unstable. To circumvent this limitation, native Python tools such as the TkInter GUI are being studied for the generation of an executable interface for the program. There are still opportunities for optimization of the program, streamlining its processing and feeding of the database.

3. RESULTS

3.1. Graphical User Interface

A simple graphical user interface (GUI) has been developed through Microsoft Excel 2016 and is presented in Figures 2 to 3. This tool is familiar to most users, facilitating engineering analysis. The GUI currently has 4 analysis panels that focus on: 1. Pressure forces, 2. Aerothermodynamics of the freestream, 3. Aerothermodynamics of the boundary layer, and 4. Summary of critical aerothermodynamic events in the hypersonic engine geometry . Navigation between the panels is done by buttons.

By these panels, the user can analyze and permute the database with the help of 4 filters, which segment the data in, respectively: 1. Simulated Scramjet, 2. Scramjet Ramp, 3. Cruise Mach, 4. Cruise altitude.

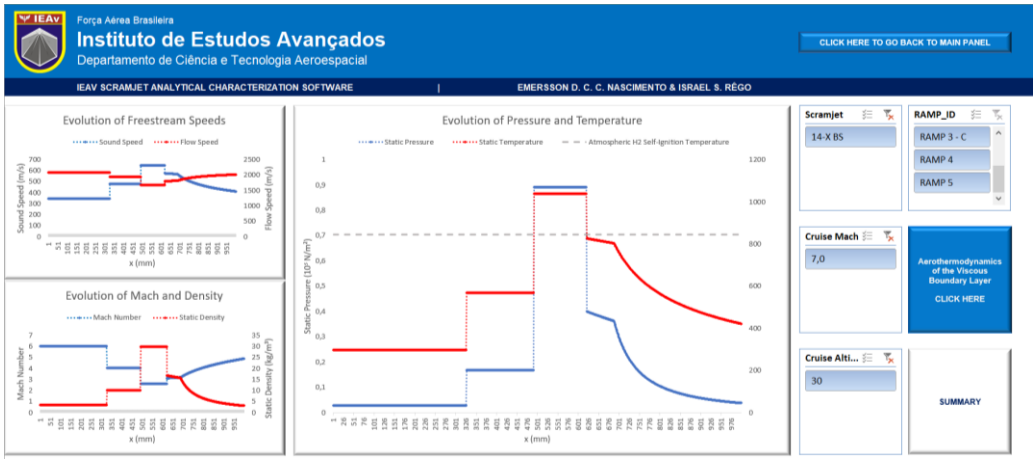

Figure 2 - GUI Secondary Panel displaying freestream analysis.

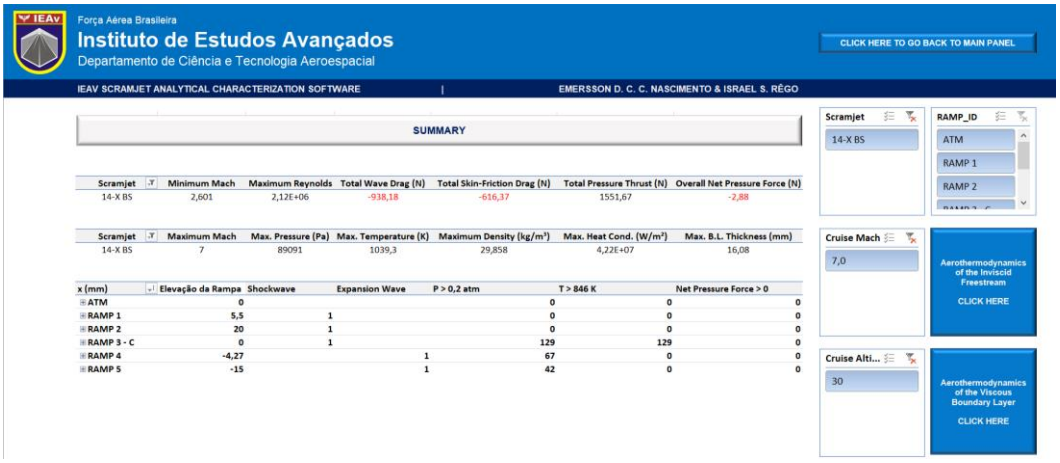

Figure 3 - GUI Summary Panel displaying main aerothermodynamics information.

3.2. Shock and Expansion Waves Characterization

The shock waves and expansion waves along the 14-X BS Scramjet freestream are characterized in Figure 4.

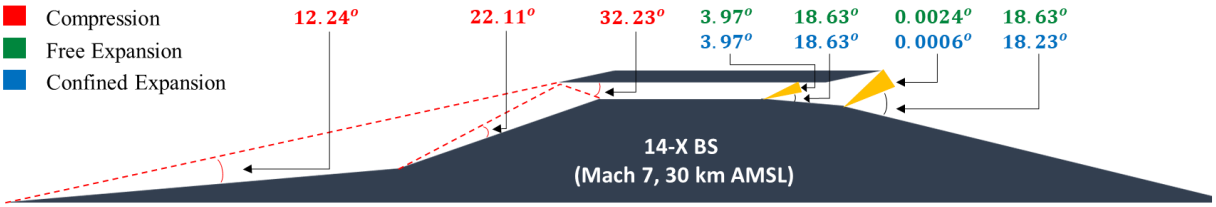

Figure 4 - 14-X BS shock and expansion waves characterization at Mach 7, 30 km AMSL.

3.3. Aerothermodynamic characterization of the non-viscous nucleus

The air-thermodynamic properties of the 14-X BS free flow were characterized, as shown in Figures 5 to 7.

It is noted that in the two compression ramps, there is an intense decrease in velocity, converted into an equally intense increase in density, pressure and temperature. It is also observed the formation of two levels, corresponding respectively to the action of the first two shock waves. Then, a new threshold is formed by the action of the third shock wave under shock-on-lip-on-corner condition (Curran and Murthy, 2000). This level corresponds to the combustor region, where the maximum values of pressure, temperature and density are observed, concomitantly with the slower (still supersonic) freestream velocity, as expected (Curran and Murthy, 2000).

At the downstream, we observe the formation of two new levels, continuous with each other, due to the action of the two expansion waves at the beginning of each expansion ramp. In this region, there is a logarithmic increase of the flow velocity, accompanied by a logarithmic decrease in pressure, temperature and density, also as expected (Curran and Murthy, 2000). Note that the aerothermodynamic variation of the flow is more intense in the second expansion ramp, due to its higher elevation.

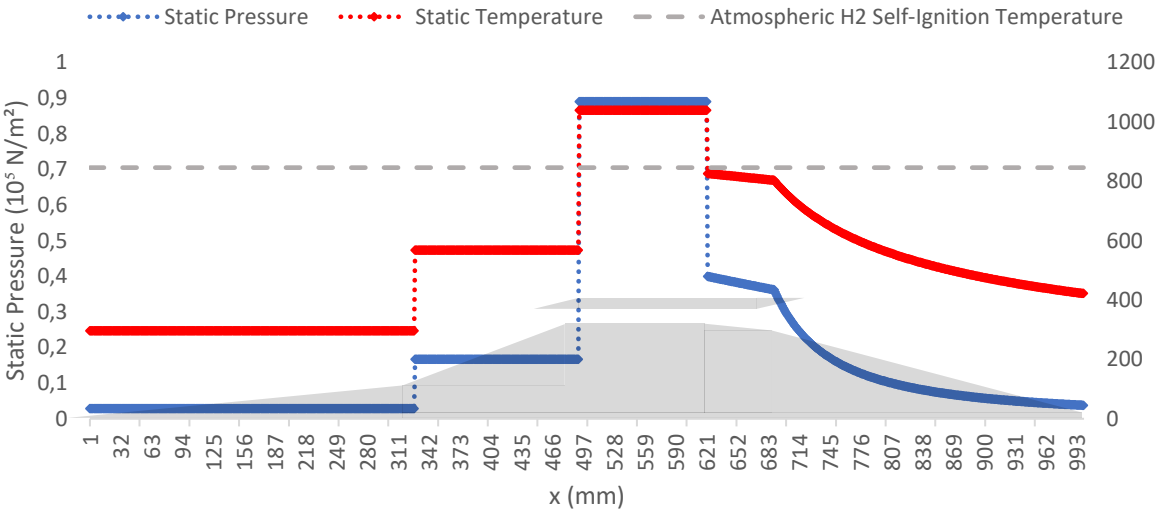

Figure 5 – Freestream Static Pressure vs Static Temperature. Mach 7 at 30 km altitude.

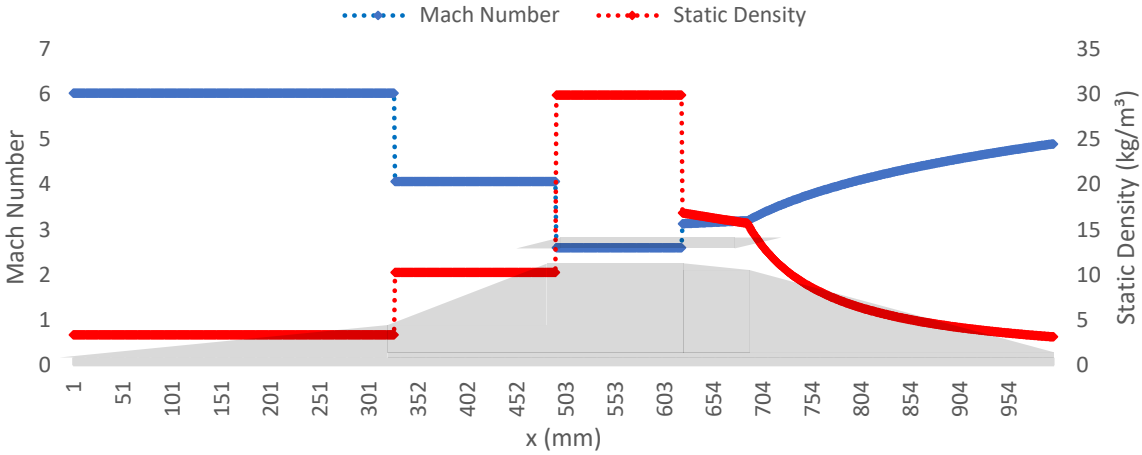

Figure 6 - Freestream Mach Number vs Static Density. Mach 7 at 30 km altitude.

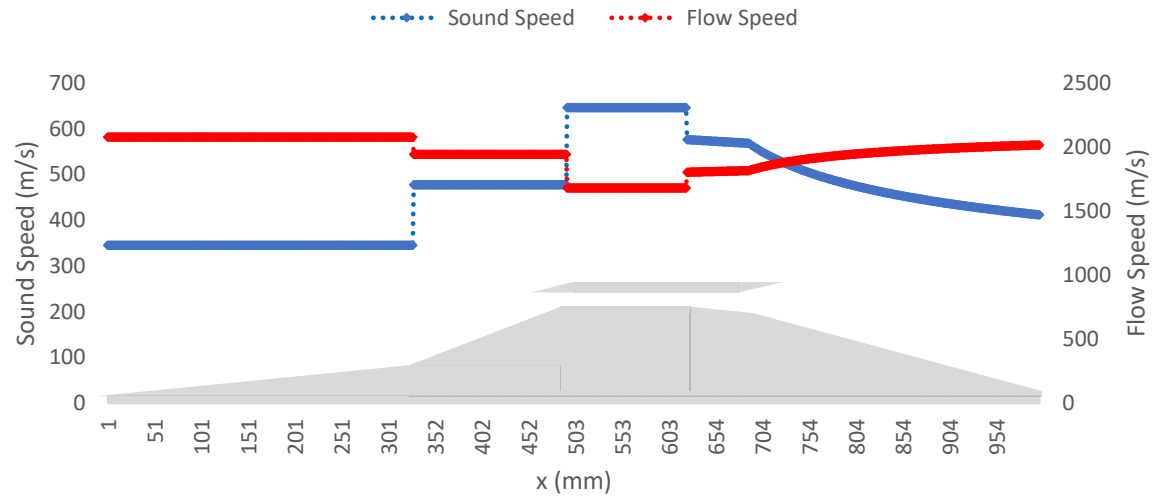

Figure 7 - Freestream Sound Speed vs Flow Speed. Mach 7 at 30 km altitude.

3.4. Aerothermodynamic characterization of the viscous nucleus

The aerothermodynamic properties of the 14-X BS boundary layer were characterized, as shown in Figures 8 to 10.

It can be seen from Figure 8 that the flow has a predominantly laminar characteristic along the hypersonic engine, being slightly more turbulent in the combustor and in the first expansion ramp, with a maximum of $Re_x \approx 2{,}1\ x\ 10^6$. This feature favors supersonic fuel mixing and the diffusion of radicals in the flow. Therefore, it favors supersonic combustion.

It can also be observed that the thickness of the boundary layer accompanies the laminarity in the first four ramps, being larger, the larger the Reynolds number. However, in the last expansion ramp, there is a discontinuity for $\delta(Re_x = 1{,}0\ x\ 10^6)$, due to the adopted model, which does not consider a transition region. Thus, a more refined mathematical model is needed for transition regions. Nonetheless, considering the discontinuity of the layer between the expansion ramps, due to the occurrence of expansion wave, this result already allows an adequate assumption that the thickness reaches its maximum at the first final expansion ramp, in the value of $\delta_{máx} \approx 14{,}7\ mm$.

At the last ramp, the layer continues to expand, although the laminarity decreases. This behavior is due to the extension of the ramp, which has a greater influence than the square root of the Reynolds number.

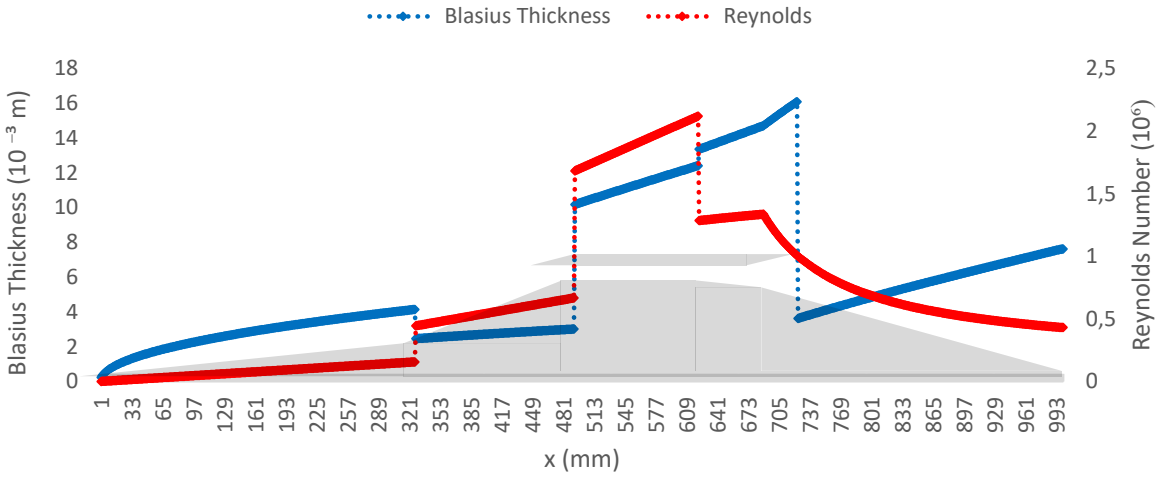

Figure 8 – Boundary Layer Thickness vs Reynolds Number. Mach 7 at 30 km altitude.

From Figure 9, it is verified that the local friction coefficient follows the freestream velocity, reaching its maximum on the first ramp and its minimum in the combustor. This behavior is consistent since the higher the velocity of the laminar freestream, the greater the effects of viscosity and friction between the current lines close to the wall.

The thermal conduction between the interface of the boundary layer and the freestream is shown in Figure 10. In this, it is observable that the conduction follows the freestream temperature. Its maximum occurs in the combustor, which also favors the energy transfer in the flow, favoring the supersonic combustion.

We note from this results that the hypersonic engine is well sized to allow adequate aerothermodynamic conditions for the supersonic combustion in its combustor. The analyzes in the following section of this report verify their suitability for the drag effects generated by the pressure and friction of the flow along the scramjet.

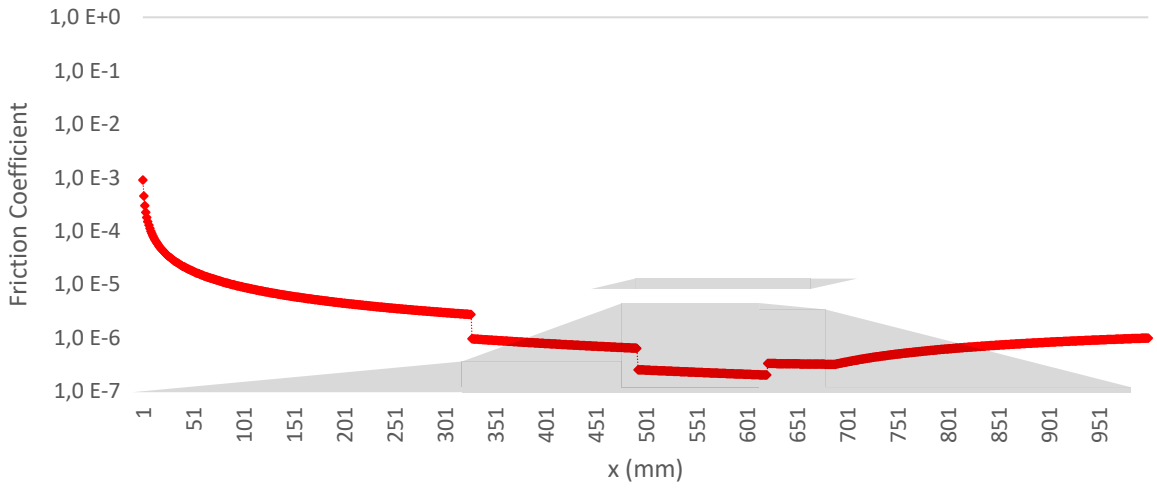

Figure 9 – Boundary Layer Friction Coefficient. Mach 7 at 30 km altitude.

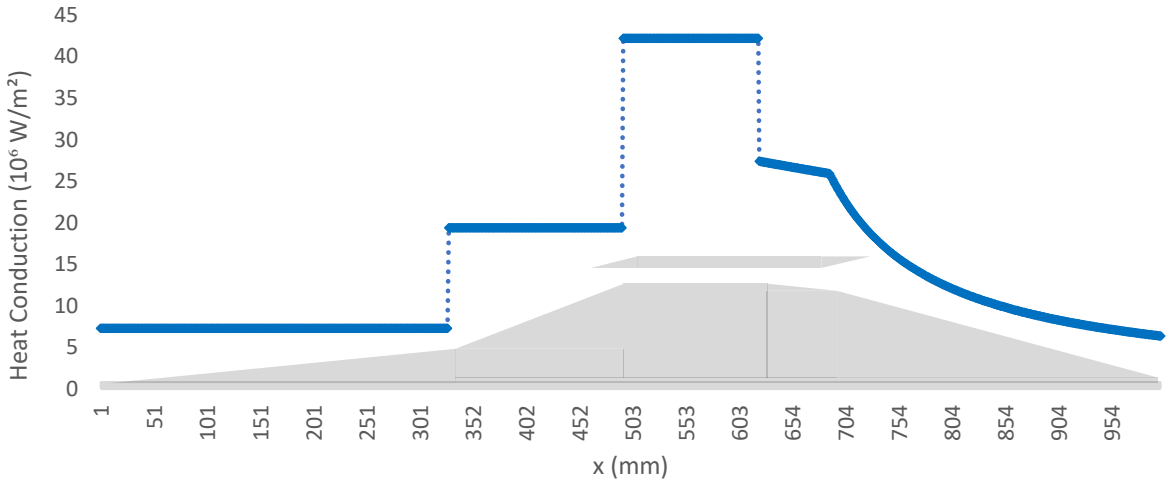

Figure 10 – Boundary Layer and Freestream Interface Heat Conduction. Mach 7 at 30 km altitude.

3.5. 1.1. Aerothermodynamic characterization of the forces of interest

The evolution of the horizontal forces is presented in Figures 11 to 13. It is emphasized that any pressure of the flow in the expansion ramps exerts pressure force on the structure of the scramjet, favoring its movement. For this reason, it is considered as pressure thrust, and represented as positive. On the other hand, if the same mechanism occurs for the direction opposite to the scramjet movement, the acting force is considered as wave drag, and represented as negative.

The greatest generation of wave drag occurs in the second compression ramp, being, concomitantly, the ramp of higher elevation and higher pressure. The combustor does not generate wave drag because it has no vertical projection.

Although the expansion ramps have a shorter length than the compression ramps, the high flow pressure coming from the combustor, combined with effects of ramp elevation and confined expansion, generates a pressure thrust significantly greater than the wave drag. Concomitantly, the skin-friction drag reaches its maximum on the first ramp, and minimum in the combustor. After the combustor, it increases back on the expansion ramps.

This study analyzed the resultant force between wave drag and pressure thrust, in Figure 11, along the length of the engine and identified that the resultant only becomes positive on the last scramjet ramp at $x \approx 778$ mm from the start of the scramjet. This view allows us an important statement about engine sizing: considering only wave drag and pressure thrust, the scramjet would reach its balance of forces if its last ramp was only approximately 89 mm in length, almost 3,5 times less than the projected. However, this statement, while giving us valuable insight to overcome wave drag, is incomplete from the engineering point of view, as it does not consider skin-friction drag.

Similarly, a new analysis, in Figure 12, that considered only skin-friction drag and pressure thrust identified that the scramjet would reach its force balance at $x \approx 705$ mm from the start of the scramjet, i.e., if its last ramp was only about 16 mm long, almost 20 times less than the projected.

However, considering all of the actuating forces under study, in Figure 13, the force balance occurs only at the end of the last ramp, where the resulting force tends to approximately -2.2 N. A suitable scramjet dimensioning is thus confirmed.

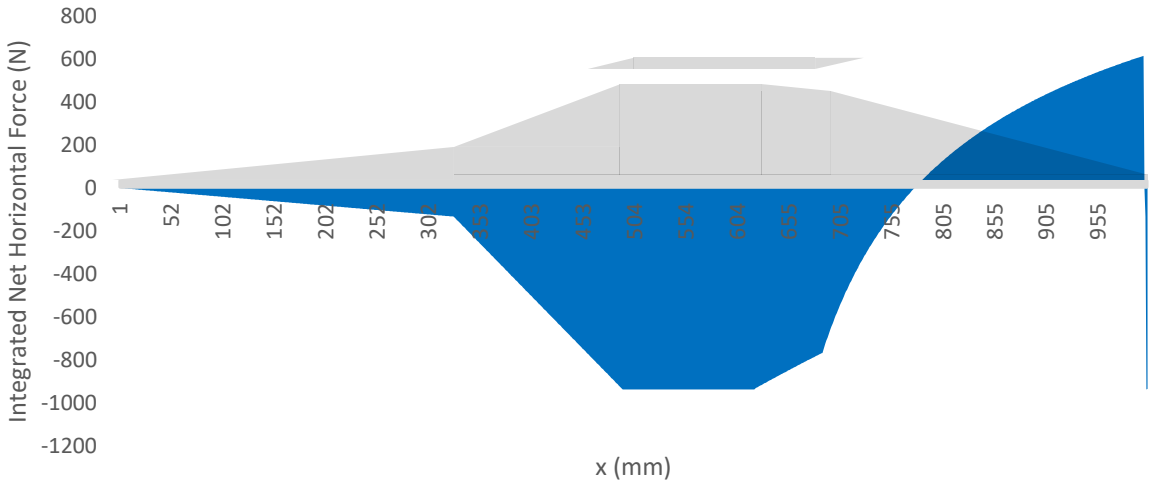

Figure 11 – Wave Drag vs Pressure Force. Mach 7 at 30 km altitude.

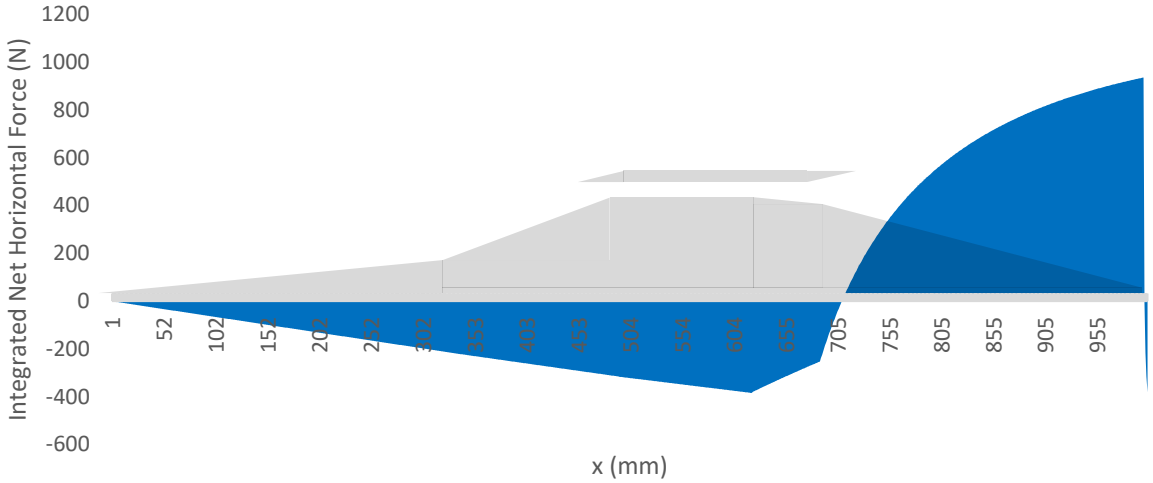

Figure 12 - Skin-Friction Drag vs Pressure Force. Mach 7 at 30 km altitude.

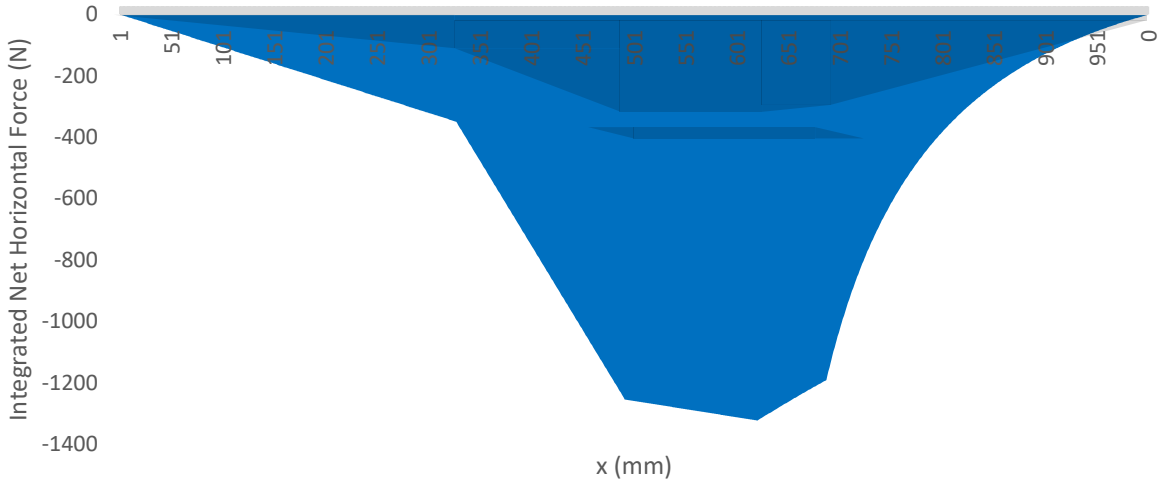

Figure 13 - Wave Drag vs Skin-Friction Drag vs Pressure Force. Mach 7 at 30 km altitude.

3.6. Critical Aerothermodynamic Results

The main critical aerothermodynamic results for the 14-X BS Scramjet at Mach 7 and 30 km altitude are summarized at Tables 1 and 2.

Table 1 – Main Aerothermodynamic Properties of the 14-X BS Scramjet. Mach 7 at 30 km altitude.

Lowest Mach	Highest Reynolds	Boundary Layer Thickness (mm)	Highest Temperature (K)	Highest Pressure (atm)	Highest Density (kg/m³)
2,601	2,12 x10^6	14,7	1039,3	0,89	29,858

Table 2 - Main Aerothermodynamic Forces of the 14-X BS Scramjet. Mach 7 at 30 km altitude.

Wave Drag (N)	Skin-Friction Drag (N)	Pressure Thrust (N)	Horizontal Net Force (N)
-938,2	-615,7	1551,7	-2,2

The highest temperature exceeds 800K thorough the combustor. At this temperature, the H_2, used as fuel in this scramjet, auto-ignition for low pressures is widely studied in literature (DEREVYAGO, 2009). The flow is completely supersonic, validating the engine as a scramjet.

4. CONCLUSIONS

At the present stage of development, a preliminary theoretical-computational modeling was developed, allowing the development of the beta version of the IEAv Scramjet Analytical Characterization Software and its graphical user interface. With the results obtained for the Scramjet 14-X BS at Mach 7 and 30 km altitude, the elaborated modeling was validated for its propose and the dimensioning of the hypersonic motor was analyzed as a function of its aerothermodynamics.

Non-viscous and viscous nuclei of the 14-X BS hypersonic engine resident flow were characterized as a function of their main aerothermodynamic properties, obtaining all preliminary desired outputs for the software. While there are many opportunities ahead for refinement, the prospects for developing a full version of the software are good.

5. FUTURE WORK

Among the future works projected for this research are:

- Modeling and coding for mixed flows (laminar and turbulent);
- Modeling and coding to include supersonic combustion effects;
- Coding Optimization;
- Simulation of new sets of cruising altitude and Mach de Cruzeiro;
- Simulation of new geometries;
- Comparison of simulated results with experimental results;
- Creation of an Artificial Intelligence to identify the best mission architectures for each geometry of flat plate scramjets;
- Creation of an Artificial Intelligence to identify the best geometries of flat plate scramjets for each mission architecture.

6. REFERENCES

ANDERSON, J. D. 2003. Modern Compressible Flow, The Historical Perspective McGraw-Hill, Inc.

ANDERSON, J. D. 2006. Hypersonic and high-Temperature Gas Dynamics. 2nd ed. AIAA. ISBN-13: 987-1-56347-780-5.

ANDERSON, J. D. 2011. Fundamentals of Aerodynamics. New York: McGraw-Hill, 1106 p. Fifth Edition.

BLUE ORIGIN. Technology. 2017. EUA. Website. Available at: < https://www.blueorigin.com/technology> Last Access: 26/05/2011.

CARDOSO, R. L. et al. Brazilian 14-X S Hypersonic Scramjet Aerospace Vehicle Dimensional Design at Mach Number 7. In: COBEM, 22, 2013, Ribeirão Preto – SP, Anais.. Ribeirão Preto-SP: ABCM, ISSN: 2176-5480. p.8396-8405

CARDOSO, R. L.; Estudo Aerodinâmico e Dimensional para Manufatura do Veículo Hipersônico Aeroespacial 14-X BS. 2012. Trabalho de Graduação. FATEC de São José dos Campos, SP.

COSTA, F. J. et al. Brazilian 14-X Hypersonic Waverider Scramjet Aerospace Vehicle Dimensional Design at Mach Number 10. In: COBEM, 22, 2013, Ribeirão Preto – SP, Ribeirão Preto-SP: ABCM, ISSN: 2176-5480. p.8396-8405

CURRAN, E.T. e MURTHY, S.N.B. Scramjet Propulsion. Progress in Astronautics and Aeronautics, Vol. 189.EUA: AIAA, 2000.

DEREVYAGO A., PENYAZKOV O., RAGOTNER K., SEVRUK K. 2009. Auto-ignition of hydrogen-air mixture at elevated pressures. In: Hannemann K., Seiler F. (eds) Shock Waves. Springer, Berlin, Heidelberg. Print ISBN 978-3-540-85167-7.

GALVÃO, V. A. B.; TORO, P. G. P. Brazilian 14-X B Hypersonic Scramjet Aerospace Vehicle Analytical Theoretical Analysis at Mach Number 7. In: COBEM, 22, 2013, Ribeirão Preto – SP, Ribeirão Preto-SP: ABCM, ISSN: 2176-5480. p.1736-1747

HEISER, H. W. and PRATT, D. T (with Daley, D. H. and Mehta, U. B.), 1994. Hypersonic Airbreathing. Propulsion. Education Series. EUA. AIAA.

INDIA SPACE RESEARCH ORGANIZATION. India's Reusable Launch Vehicle-Technology Demonstrator (RLV-TD), Successfully Flight Tested. Índia. ISRO. 2016. Available at: http://www.isro.gov.in/update/23-may-2016/india%E2%80%99s-reusable-launch-vehicle-technology-demonstrator-rlv-td-successfully.. Last Access: 20/05/2016.

NASCIMENTO, E. D. C. C. et al. Development of a Laser Igniter for the Scramjet Engine of the 14-X Hypersonic Aerospacecraft. In: COBEM, 22, 2013, Ribeirão Preto – SP, Anais.. Ribeirão Preto-SP: ABCM, ISSN: 2176-5480. p.704-713

NASCIMENTO, E. D. C. C., REGO, I. S. Arrasto de Onda do Veículo Hipersônico 14-X BS nivelado a Mach 7 e altitude de 30 Km: Modelagem Preliminar. Em IV SICTI, 2016, São José dos Campos – SP. Anais.. Simp. Iniciac. Cient. Tecnol. IEAv, v.1, p.30-35, ago/2015-jul/2016

NASCIMENTO, E.D.C.C. e REGO, I. S. 2017. Estudo do Arrasto de Onda do Veículo Hipersônico 14-X BS nivelado a Mach 7 e Altitude de 30 km. Formulário de Encaminhamento de Relatório Final – Iniciação Científica. IEAV. São José dos Campos, SP.

NATIONAL AERONAUTICS AND SPACE ADMINISTRATION. US Standard Atmosphere, 1976. Washington, D.C., EUA. NOAD, NASA, USAF. 1976. Available at: <http://ntrs.nasa.gov/archive/nasa/casi.ntrs.nasa.gov/19770009539.pdf>. Last Access: 28/05/2016

SPACEX. Falcon 9 Launch Vehicle: Payload User's Guide - Revision 2. California, EUA. SpaceX. 2015. Disponível em: <http://www.spacex.com/sites/spacex/files/falcon_9_users_guide_rev_2.0.pdf>. Acesso em: 20/05/2016.

VAN DRIEST, F. R. 1952. Investigation of Laminar Boundary Layer in Compressible Fluids Using the Crocco Method. NACA TN 2597.

WHITE, F. M. Fluid Mechanics. Porto Alegre: McGraw-Hill e AMGH Editora Ltda, 2011, 880 p. 6ª ed.

7. RESPONSABILIDADE AUTORAL

The authors are the only ones responsible for the content of this work.

8. ACKNOWLEDGMENTS

This work was supported by the Institute for Advanced Studies of the Brazilian Air Force.